Inventory of Supplemental Information

I. Supplemental Figures

Supplemental Figure S1-S2 is related to main Figure 1.

Supplemental Figure S3-S6 is related to main Figure 2.

Supplemental Figure S5 is related to main Figures 2, 4, 5, 7.

Supplemental Figure S7 is related to main Figure 3.

II. Supplemental Tables

Supplemental Table S1 includes all primer sequences used in the study.

Supplemental figure legends

Figure S1. Characterization of p54^{nrb} methylation (related to Figure 1). (A) Identification of p54^{nrb} methylation by PRMTs. The indicated PRMTs were used to methylate p54^{nrb}. The methylated proteins were separated by SDS-PAGE, transferred to a PVDF membrane, and visualized by fluorography. The same membrane was subjected to Ponceau staining to verify substrate equal loading. (B) Characterization of p54^{nrb} methylation by CARM1. Top, a schematic view of regions of p54^{nrb} fused to his-tag for deletion analysis. Bottom, purified his-tagged p54^{nrb} truncations were incubated with recombinant GST-CARM1 in the presence of [^{3}H]AdoMet, separated by SDS-PAGE, and the methylated proteins visualized by fluorography (bottom right panel). A duplicate substrate gel was Coomassie stained to demonstrate loading (bottom left panel). Red dots indicated the expression of p54^{nrb} truncations.

Figure S2. p54^{nrb} is methylated by CARM1 (related to Figure 1). (A) CARM1 was knocked down in HeLa and HEK 293 cells, as validated by Western blotting (WB). Actin was used as a loading control. (B) Flag- p54^{nrb} was expressing in scramble and CARM1 KD HeLa cells. The top is the silver staining of IP complex. The bottom is the western blotting analysis of IP efficiency. The Flag-p54^{nrb} IP samples were subjected to MS. (C) The sequence of human p54^{nrb}. Amino Acids highlighted by blue indicate the RRM domains, while Amino Acids highlighted by red indicate the Coiled-coil domain. All Arginines (R) were underscored. R73, R184 and R207 were present in both scramble and CARM1 knockdown Flag-p54^{nrb} IP samples, while R357, R365 and R378 were present in the scramble, but not the CARM1 knockdown, Flag-p54^{nrb} IP sample. (D) Hybrid mass spectrometry identified Arg357, Arg365 and Arg378 are major methylation sites on p54^{nrb} by CARM1 in HeLa cells.

Figure S3. CARM1 deficiency suppresses *egfp*-IR*Alu*s expression (related to Figure 2). (A) CARM1 KD suppresses EGFP expression of *egfp* mRNA containing IR*Alu*s in its 3'-UTR. IR*Alu*s and *Alu* from the 3'-UTR of *Lin28* were inserted into the 3'-UTR of *egfp* mRNA (Chen et al. 2008). Stable HeLa cell lines with the scramble shRNA treatment and CARM1 KD were transfected with the indicated plasmids and fluorescence observed 24 h after transfection. (B) The expression of EGFP and transcripts of *egfp* from the same batch of transfected HeLa cells as described (A) were investigated by WB by probing with anti-EGFP antibody; and by NB by probing with a Dig-labeled *egfp* fragment. Actin was used as loading control for WB. Equivalent amounts of total RNAs were loaded for NB as indicated by 28S and 18S rRNAs. (C) The relative translation efficiency (the relative intensity of each corresponding band from WB and NB shown in panel B) of *egfp-Alu* and *egfp-IRAlus* mRNA in scramble and CARM1 KD cells.

Figure S4. CARM1 deficiency enhances nuclear retention of mRNAs containing IR*Alu*s in HEK293 cells (related to Figure 2). (A) CARM1 KD suppresses EGFP expression of *egfp* mRNA containing IR*Alu*s in its 3'-UTR. IR*Alu*s and *Alu* from the 3'-UTR of *Nicn1* were inserted into the 3'-UTR of *egfp* mRNA (Chen et al. 2008). Stable HEK293 cell lines with the scramble shRNA treatment and CARM1 KD were transfected with the indicated plasmids and fluorescence observed 24 h after transfection. (B) The expression of EGFP and transcripts of

egfp from the same batch of transfected HEK293 cells as described in (A) were investigated by WB by probing with anti-EGFP antibody. Actin was used as loading control for WB. (C) CARM1 deficiency significantly enhances the nuclear retention of *egfp* mRNA with IR*Alu*s. The cytoplasmic and nuclear RNAs were isolated from HEK293 cells with the indicted treatment and then were used for RT-qPCR analysis. Note that the sub-cellular distributions of both the co-transfected *mcherry* and the endogenous *actin* mRNAs exhibited little changes in the scramble and CARM1 KD HEK293 cells. (D) CARM1 KD enhances the nuclear retention of other endogenous mRNAs with IR*Alu*s in HEK293 cells. RT-qPCR analyzed a number of other endogenous mRNAs with IR*Alu*s using nuclear and cytoplasmic fractionated RNAs. Primers to detect IR*Alu*s RNAs were designed in the downstream of IR*Alu*s in 3'-UTRs (Figure S5). The relative subcellular distribution of each IR*Alu*s RNA was normalized to the relative amount of *malat1* RNA. In (C)(D), SD was obtained from three independent experiments. (*)P<0.05; (**)P<0.01; n=3.

Figure S5. A schematic drawing of transcripts containing a pair of IR*Alu*s in their 3'-UTRs (related to Figures 2, 4, 5 and 7). Black bars represent exons, thin black lines represent introns. The position and direction of *Alu* elements in 3'-UTRs were shown in white arrows. The primer set recognizing each transcript is labeled as a thick blue line underneath.

Figure S6. CARM1 KD enhances the nuclear retention of endogenous mRNAs with IR*Alu*s in their 3'-UTRs (related to Figure 2). (A) RT-qPCR quantitations of endogenous mRNAs with IR*Alu*s in total, cytoplasmic and nuclear fractionations. The level of each cellular mRNA was normalized to the level of *actin* mRNA in scramble and CARM1 KD HeLa cells. SD was obtained from three independent experiments. (*)P<0.05; (**)P<0.01; n=3. T, total RNA; C, cytoplasmic RNAs; N, nuclear RNAs. (B) CARM1 KD promotes the nuclear retention of endogenous *icmt* mRNA. Top, cytoplasmic and nuclear RNA fractionation of scramble and CARM1 KD HeLa cells followed by NB to detect *icmt* mRNA. $tRNA^{lys}$ and *actin* revealed a successful cytoplasmic and nuclear fractionation. Equivalent amounts of RNA from different compartments were loaded as indicated by 28S and 18S rRNAs. Bottom, the relative subcellular distribution of the *icmt* mRNA was quantified from top panels by Image J and was presented by the normalization to the *actin* mRNA in each subcellular compartment.

Figure S7. Visualization of *mcherry-IRAlus* expression after $p54^{nrb}$ and CARM1 knockdown (related to Figure 3). (A) While CARM1 KD suppresses mcherry expression of *mcherry* mRNA containing IR*Alu*s in its 3'-UTR, knockdown of $p54^{nrb}$ enhances mcherry expression of the same plasmid. (B) Expression of WT CARM1 but not the catalytic inactive mutant E266Q CARM1 in CARM1 KD HeLa cells could rescue the expression of mcherry mRNAs with IR*Alu*s in its 3'-UTR. (C) A schematic drawing for the nuclear retention regulation of *mcherry* mRNAs with IR*Alu*s in its 3'-UTR under different conditions. See text for details.

Supplemental figures

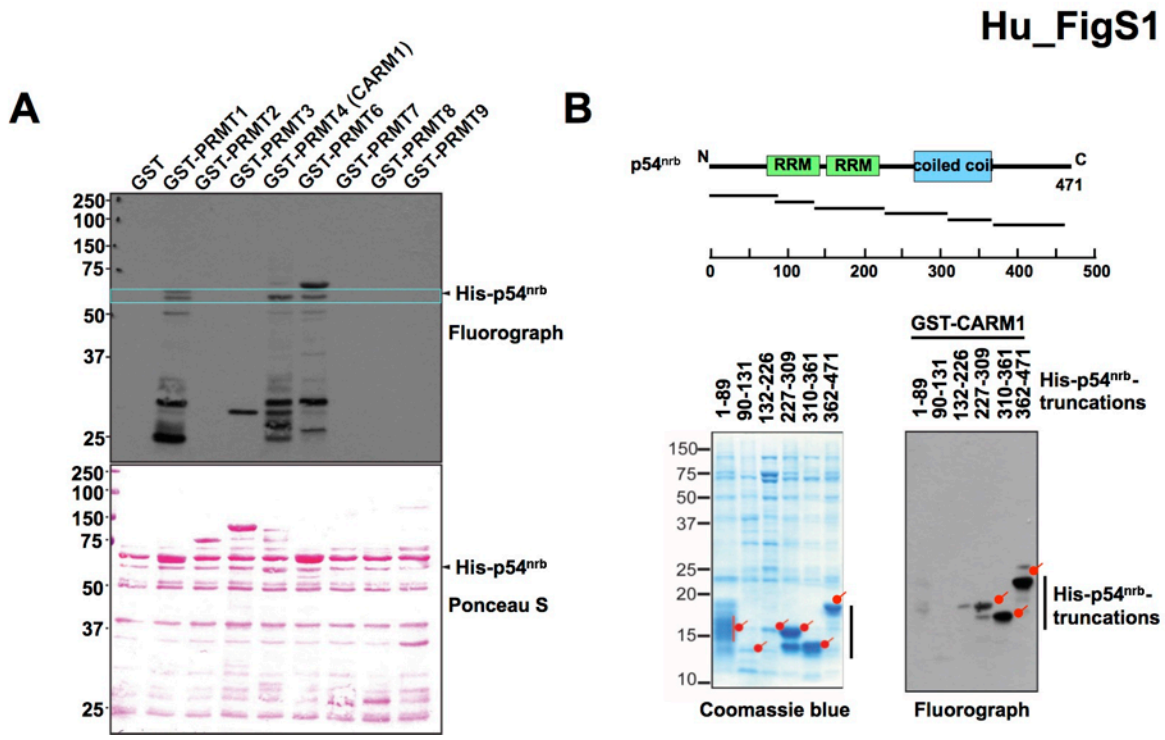

Hu_FigS2

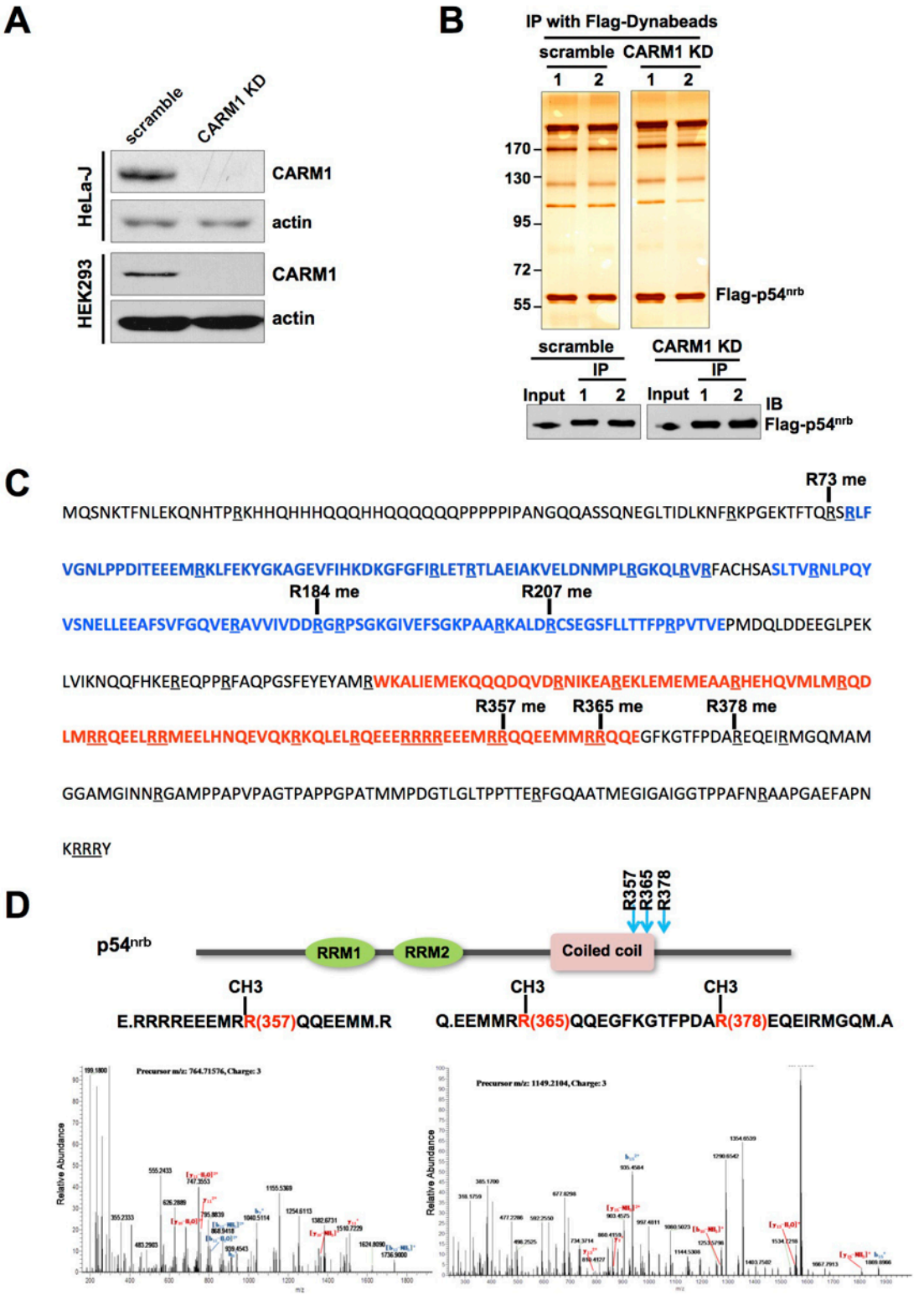
A
scramble
CARM1 KD
HeLaJ
CARM1
actin
HEK293
CARM1
actin
B
IP with Flag-Dynabeads
scramble
CARM1 KD
1
2
1
2
170
130
95
72
55
Flag-p54nrb
scramble
CARM1 KD
IP
IP
Input 1 2
Input 1 2
IB
Flag-p54nrb
C
R73 me
MQSNKTFNLEKQNHTPRKHHQHHHQQQHHQQQQQQPPPPPIPANGQQASSQNEGLTIDLKNFRKPGEKTFTQRSRLF
VGNLPPDITEEEMRKLFEKYGKAGEVFIHKDKGFGFIRLETRTLAEIAKVELDNMPLRGKQLRVRFACHSASLTVRNLPQY
R184 me
R207 me
VSNELLEEAFSVFGQVERAVVIVDDRGRPSGKGIVEFSGKPAARKALDRCSEGSFLLTTFPRPVTVEPMDQLDDEEGLPEK
LVIKNQQFHKEREQPPRFAQPGSFEYEYAMRWKALIEMEKQQQDQVDRNIKEAREKLEMEMEAARHEHQVMLMRQD
R357 me
R365 me
R378 me
LMRRQEELRRMEELHNQEVQKRKQLELRQEEERRRREEEMRRQQEEMMRRQQEGFKGTFPDAREQEIRMGQMAM
GGAMGINNRGAMPPAPVPAGTPAPPGPATMMPDGTLGLTPPTTERFGQAATMEGIGAIGGTPPAFNRAAPGAEFAPN
KRRRY
D
R357
R365
R378
p54nrb
RRM1
RRM2
Coiled coil
CH3
CH3
CH3
E.RRRREEEMRR(357)QQEEMM.R
Q.EEMMRR(365)QQEGFKGTFPDAR(378)EQEIRMGQM.A
Precursor m/z: 764.71576, Charge: 3
Precursor m/z: 1149.2104, Charge: 3
Relative Abundance
Relative Abundance

Hu_FigS3

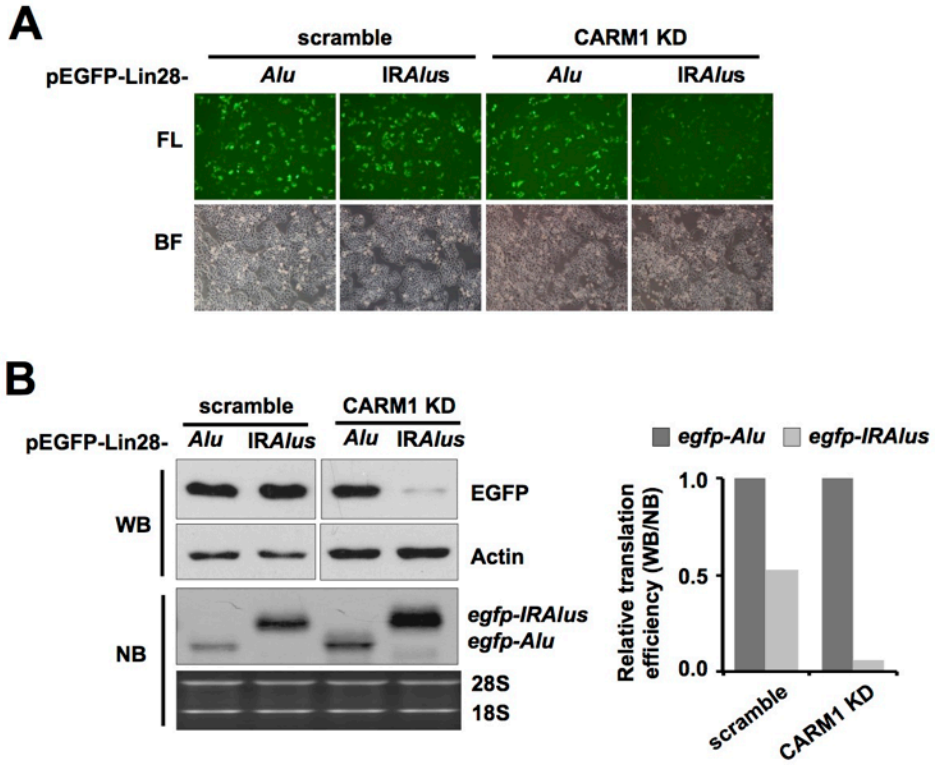
A
scramble
CARM1 KD
pEGFP-Lin28-
Alu
IRAlus
Alu
IRAlus
FL
BF
B
scramble
CARM1 KD
pEGFP-Lin28-
Alu
IRAlus
Alu
IRAlus
WB
NB
EGFP
Actin
egfp-IRAlus
egfp-Alu
28S
18S
egfp-Alu
egfp-IRAlus
Relative translation efficiency (WB/NB)
1.0
0.5
0.0
scramble
CARM1 KD

Hu_FigS4

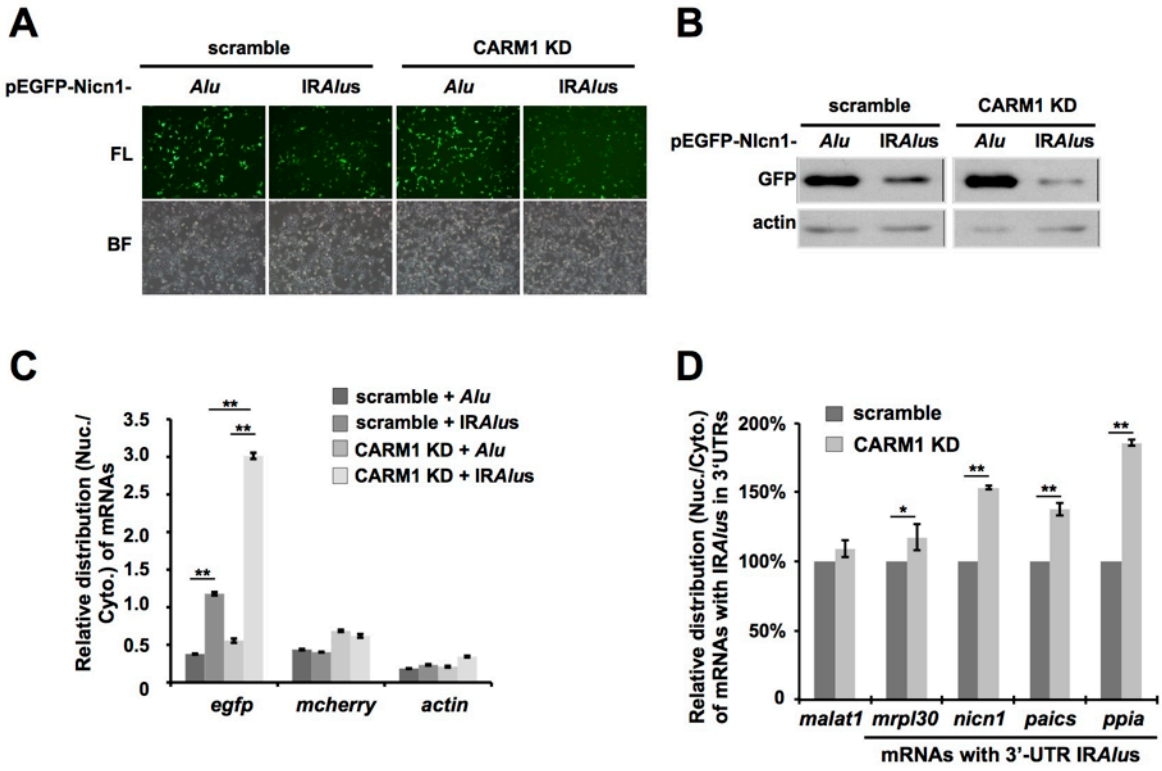
A
scramble
CARM1 KD
pEGFP-Nicn1-
Alu
IRAlus
Alu
IRAlus
FL
BF
B
scramble
CARM1 KD
pEGFP-NIcn1-
Alu
IRAlus
Alu
IRAlus
GFP
actin
C
scramble + Alu
scramble + IRAlus
CARM1 KD + Alu
CARM1 KD + IRAlus
Relative distribution (Nuc./ Cyto.) of mRNAs
3.5
3.0
2.5
2.0
1.5
1.0
0.5
0
**
**
**
egfp
mcherry
actin
D
scramble
CARM1 KD
Relative distribution (Nuc./Cyto.) of mRNAs with IRAlus in 3'UTRs
200%
150%
100%
50%
0
*
**
**
**
malat1
mrpl30
nicn1
paics
ppia
mRNAs with 3'-UTR IRAlus

Hu_FigS5

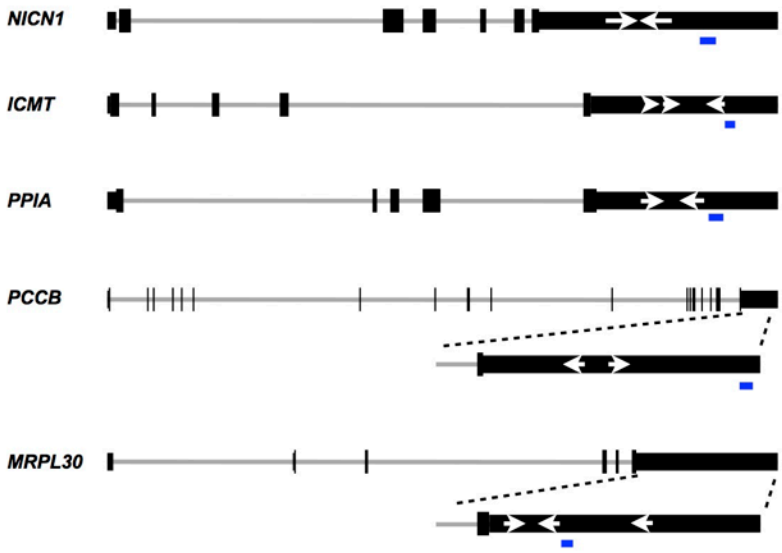

Hu_FigS6

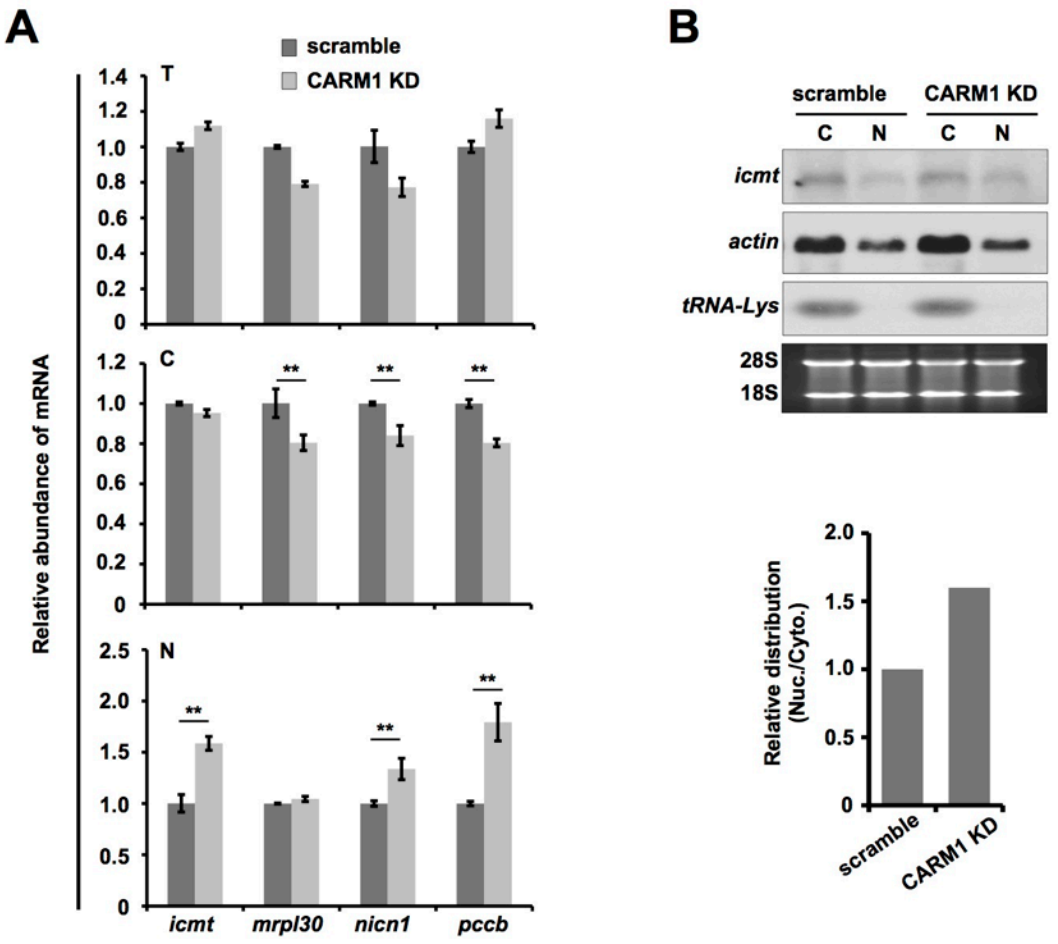
A
scramble
CARM1 KD
T
C
N
Relative abundance of mRNA
1.4
1.2
1.0
0.8
0.6
0.4
0.2
0
2.5
2.0
1.5
0.5
**
icmt
mrpl30
nicn1
pccb
B
scramble
CARM1 KD
C
N
icmt
actin
tRNA-Lys
28S
18S
Relative distribution
(Nuc./Cyto.)
2.0
1.5
1.0
0.5
0
scramble
CARM1 KD

Hu_FigS7

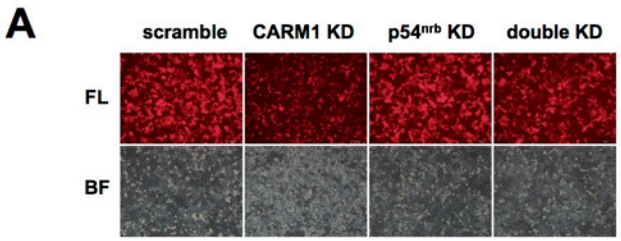
A
scramble
CARM1 KD
p54nrb KD
double KD
FL
BF

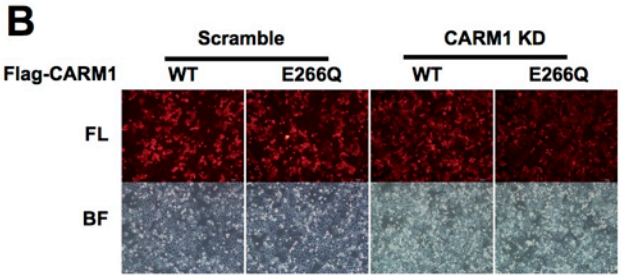
B
Scramble
CARM1 KD
Flag-CARM1
WT
E266Q
WT
E266Q
FL
BF

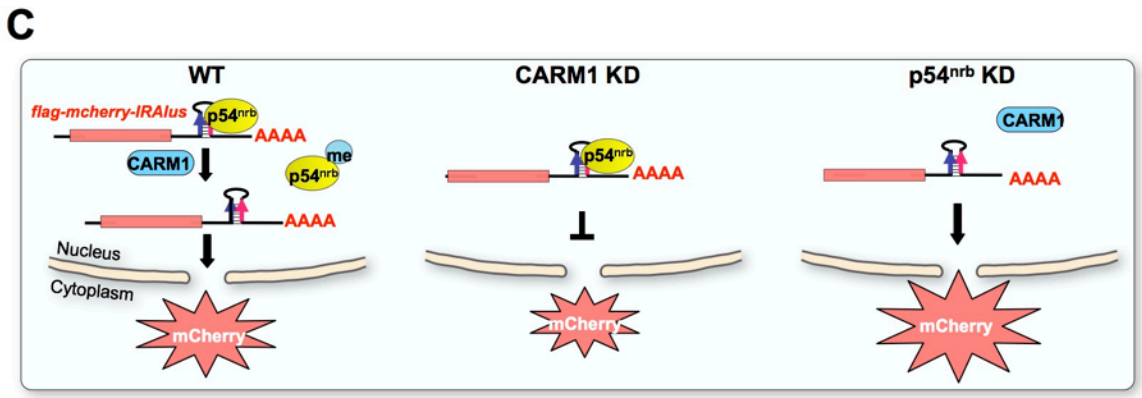
C
WT
CARM1 KD
p54nrb KD
flag-mcherry-IRAlus
p54nrb
AAAA
CARM1
me
p54nrb
AAAA
Nucleus
Cytoplasm
mCherry
p54nrb
AAAA
mCherry
CARM1
AAAA
mCherry

Supplemental Table S1. Primers used in this study.

qPCR primers for IRAlus Genes	
qNicn1-F	ACTTCATCTGCAAGGTCACTTAC
qNicn1-R	ACAGTAGTCTGTCCTCATGTGG
qPAICS-F	CGTAATTTTGGACTGCCACA
qPAICS-R	AGGTTTCATGGACAGCGAAC
qPccb-F	CGGTGTACAGCATCTGTTGG
qPccb-R	CATCTCTGCCAAAAACCACA
qMRPL30-F	GTGAGTGGCTCTTTGCATGA
qMRPL30-R	AGCTGGCATCCAGTGTTTCT
qICMT-F	CCTCACGAAAGGCTTCACTC
qICMT-R	GGCCACATCACCAATTTTCT
qPPIA-F	AGGGAAGCATATTGGGCTTT
qPPIA-R	CCTCTGCAGGGAGACTGACT

qPCR primers for NEAT1	
qNEAT1-F	TCGGGTATGCTGTTGTGAAA
qNEAT1-R	TGACGTAACAGAATTAGTTCTTACCA
qNEAT1-up-3F	GCAGTGATCAAACAAGGCTTC
qNEAT1-up-3R	TCAGTGTCCCTTAGGCTCAAA
qNEAT1-up-2F	ACGGCCTCTTCCCACTTAAT
qNEAT1-up-2R	AGGCATCGTGGTTTTGACTC
qNEAT1-up-1F	CAACAACATCCGGGAAGAAA
qNEAT1-up-1R	CAGTGTATCCCCGCTTCTCT
qNEAT1-1F	GGAGGGCCGGGAGGGCTAAT
qNEAT1-1R	CGGTCAGCCCCGTCGAGCTA
qNEAT1-2F	TCCTCCTGGTGGCCAAGACAGC
qNEAT1-2R	GCTAAGGGGCAGCGAAGGATGC
qNEAT1-3F	TTCTTCCCCTTTACAGCACA
qNEAT1-3R	TCGTTATGAAGGCAATGTGA
qNEAT1-4F	GCCACATTCTTTGCCTTCAT
qNEAT1-4R	CCCACACCTCTGGAAATTCA
qhNEAT1_2-F(qNEAT1-5F)	TGACTCTCCATTTCCCCATC
qhNEAT1_2-R(qNEAT1-5R)	TCATTTACCCGCATTTCACA
qNEAT1-6F	GCATTTTTCCTCTTTGACCA
qNEAT1-6R	GTGCTTTTTGCACCAACAAT
qhNEAT1_2-F-2(qNEAT1-7F)	TTGCAGCAACTGTCCTGAAG
qhNEAT1_2-R-2(qNEAT1-7R)	GGGTCCGGGATTATAGAGGA
qNEAT1-8F	GCCTGTTGTCCTTACACCAT
qNEAT1-8R	TAGGGCTTCCCTTCGCTATT
qNEAT1-9F	GGGGTGTCCCCTATCAGACT
qNEAT1-9R	AATGCTTTCCCATGATCCAG

qNEAT1-10F	GCCATCCGAGGAAGATGTAA
qNEAT1-10R	GGGATGTTGATGGAGTGACC
qNEAT1-11F	CCCACCTGGTAGTCCTCAGA
qNEAT1-11R	TGGGTGCCTTCTACTCATCC

Other qPCR primers	
qGFP-F	ACAAGCAGAAGAACGGCATC
qGFP-R	ACTGGGTGCTCAGGTAGTGG
qmcherry-F	CCCCGTAATGCAGAAGAAGA
qmcherry-R	GGCCTTGTAGGTGGTCTTGA
qhIFNβ-F	CAGCAGTTCCAGAAGGAGGA
qhIFNβ-R	AGCCAGGAGGTTCTCAACAA
qACTB-F	GGACTTCGAGCAAGAGATGG
qACTB-R	AGCACTGTGTTGGCGTACAG
qACTB for ChIP and NRO F	CCTCATGGCCTTGTCACACGAG
qACTB for ChIP and NRO R	GCCCTTTCTCACTGGTTCTCT
qnucleolin-F	CCTCAGCAAAGAAGGTGGTC
qnucleolin-R	GCCAGGTGTGGTAACTGCTT

Primers for NB probes	
F-Sp6-NICN1-upstream	GCGATTTAGGTGACACTATAGGACCTTTCCCAAG TGGCTCT
R-T7-NICN1-upstream	GCGTAATACGACTCACTATAGGGACCACTAGGGG ACACACAGG
F-Sp6-actin	GCGATTTAGGTGACACTATAGTGCTATCCCTGTAC GCCTCT
R-T7-actin	GCGTAATACGACTCACTATAGGGAGTACTTGCGC TCAGGAGGA
F-tRNA-Lys	GATCCGCCCGGATAGCTCAGTCGGTAGAGCATCA GCTTTTAATCTGAGGGTCCAGGG
R-tRNA-Lys	AGCTTCGCCCGAACAGGGACTTGAACCCTGGAC CCTCAGATTAAAAGTCTGATGCTCTA
F-NEAT1	GGGCCATCAGCTTTGAATAA
R-T7-NEAT1	TGAATTGTAATACGACTCACTATAGGGTCCCCATA CATGCGTGACTA

Biotin Pulldown primers	
F-T7-GFP	GCGTAATACGACTCACTATAGGGATGGTGAGCAA GGGCGAGGA
R-GFP	TTATCTAGATCCGGTGGATC
F-T7-dsEGFP	GCGTAATACGACTCACTATAGGGCACAAGTTCAG CGTGTCCG

R-T7-dsEGFP	GCGTAATACGACTCACTATAGGGGTTCACCTTGATGCCGTTC

Dig-RNA Pulldown primers	
F-T7-IR*Alu*s	GCGTAATACGACTCACTATAGGGCACGTGTCTCTAGCAAAACC
R-IR*Alu*s	ATGCTGAGCATATCTCTTGG

Plasmid	**Vector**	**Insert**	**Restriction enzyme**
pcDNA3.1(+)-flag	pcDNA3.1(+)	flag	HindII BamHI
pcDNA3.1(+)-flag-p54^{nrb}-wt	pcDNA3.1(+)-flag	full length p54^{nrb}	BamHI XhoI
pcDNA3.1(+)-flag-p54^{nrb}-mut	pcDNA3.1(+)-flag	R357,365,378K mutation of p54^{nrb}	BamHI XhoI
pcDNA3.1(+)-flag-EGFP	pcDNA3.1(+)-flag	EGFP	BamHI XhoI
pTracer-CARM1-WT	pTracer	WT CARM1	EcoRI NotI
pTracer-CARM1-E266Q	pTracer	E266Q mutation of CARM1	EcoRI NotI
pmCherry-flag-IR*Alu*s	pmCherry-C1	IR*Alu*s from pEGFP-C1-Nicn1-IR*Alu*s	EcoRI XhoI
pcDNA3.1(+)-flag-p54^{nrb}-1	pcDNA3.1(+)-flag	1-230bp of p54^{nrb}	BamHI XhoI
pcDNA3.1(+)-flag-p54^{nrb}-2	pcDNA3.1(+)-flag	54-375bp of p54^{nrb}	BamHI XhoI
pET28a-p54^{nrb}	pET28a	full length	BamHI EcoRI
pET28a-p54^{nrb}-△1	pET28a	1-89bp of p54^{nrb}	BamHI EcoRI
pET28a-p54^{nrb}-△2	pET28a	90-131bp of p54^{nrb}	BamHI EcoRI
pET28a-p54^{nrb}-△3	pET28a	132-226bp of p54^{nrb}	BamHI EcoRI
pET28a-p54^{nrb}-△4	pET28a	227-309bp of p54^{nrb}	BamHI EcoRI
pET28a-p54^{nrb}-△5	pET28a	310-361bp of p54^{nrb}	BamHI EcoRI
pET28a-p54^{nrb}-△6	pET28a	362-471bp of p54^{nrb}	BamHI EcoRI
pET28a-p54^{nrb}-R357,365K	pET28a	R357,365K mutation of p54^{nrb}	BamHI EcoRI
pET28a-p54^{nrb}-R378,383K	pET28a	R378,383K mutation of p54^{nrb}	BamHI EcoRI